KYUNGPOOK Math. J. 60(2020), 853-867
https://doi.org/10.5666/KMJ.2020.60.4.853
pISSN 1225-6951 eISSN 0454-8124

MHD Boundary Layer Flow and Heat Transfer of Rotating Dusty Nanofluid over a Stretching Surface

Radhika Manghat
Department of Mathematics, Government First Grade College, Bangalore University, Bangalore, India
e-mail : radhika.manghat@gmail.com

Siddabasappa*
Department of Mathematics, Government Science College, Bangalore University, Bangalore, India
e-mail : siddabasappa1961@gmail.com

Abstract. The aim of this study was to analyze the momentum and heat transfer of a rotating nanofluid with conducting spherical dust particles. The fluid flows over a stretching surface under the influence of an external magnetic field. By applying similarity transformations, the governing partial differential equations were trans-formed into nonlinear coupled ordinary differential equations. These equations were solved with the built-in function bvp4c in MATLAB. Moreover, the effects of the rotation parameter ω, magnetic field parameter M, mass concentration of the dust particles α, and volume fraction of the nano particles ϕ, on the velocity and temperature profiles of the fluid and dust particles were considered. The results agree well with those in published papers. According to the result the hikes in the rotation parameter ω decrease the local Nusselt number, and the increasing volume fraction of the nano particles ϕ increases the local Nusselt number. Moreover the friction factor along the x and y axes increases with increasing volume fraction of the nano particles ϕ.

1. Introduction

The study of nanofluids represents a new scientific field in which innovative applications have been created. Choi [2] was the first person who visualized the concept of nanofluids. While working on the micro channel liquid nitrogen cooling

* Corresponding Author.
Received January 18, 2019; accepted July 21, 2020.
2010 Mathematics Subject Classification: 80A20.
Key words and phrases: boundary layer flow, dusty nanofluid, heat transfer, magnetic field parameter, rotation parameter, stretching surface.

system, he tried to develop a heat transfer fluid that has a high thermal conductivity. To enhance the thermal conductivities of fluids, he used Maxwell's [9] concept in which metallic particles are added to base fluids. The new heat transfer fluids are created by dispersing nano meter sized particles of, for example, metals or metal oxides into base fluids such as water or ethylene glycol. Compared to conventional heat transfer fluids, nanofluids have many more advantages. They exhibit an improved heat transfer rate, stability, reduced pumping power, minimal clogging, high thermal diffusivity and high viscosity. The study of boundary layer flows over stretching sheets is important for several industrial applications such as glass fiber production, wire drawing, paper production, extrusion of plastic and rubber sheets, metal spinning, continuous casting, whirling of fibers, and cooling of plastic films and micro chips. In addition, they are applied in cancer therapy. Iron based nanoparticles are used as delivery vehicles for drugs or radiation in cancer patients. Furthermore knowledge about the flow of rotating fluids is important for the chemical industry, geophysical fluid dynamics, nuclear reactors, mechanical nuclear engineering, centrifugal filtration, biomedical spin coating, rotational viscometers, material management, conveyors, centrifugal machinery and radiators. They are applied for rotating machinery, lubrication, oceanography, computer storage devices, crystal growth processes and in many more engineering areas. In [3] the boundary layer flow due to a stretching sheet was analytically studied. The author assumed that the velocity of the sheet varies linearly with the distance from the slit. Sakiadis [12] studied the boundary layer behavior on continuous solid surfaces. Moreover Ferdows [4] investigated the boundary layer flow past an unsteady stretching surface in a nanofluid under the effects of suction and viscous dissipation with the Nachtsheim-Swigert shooting technique and Runge- Kutta sixth order iteration scheme. The author found that the thermal boundary layer thickness increases with increasing temperature. Gireesha et al [5, 6] studied the heat and mass transfer in a nanofluid film on an unsteady stretching surface and the boundary layer flow and heat transfer of a dusty fluid over a stretching vertical surface. In addition they numerically investigated the effect of the suspended particles on the boundary layer flow and heat transfer characteristics of a viscous nanofluid in a porous medium over a stretching sheet. Sandeep [11] et al analyzed the momentum and heat transfer behavior of an MHD nanofluid with conducting dust particles flowing past a stretching surface in the presence of a certain volume fraction of dust particles. The author applied a Runge-Kutta based shooting technique. The increasing interaction between the fluid and particle phase increased the heat transfer rate and reduced the friction factor. Preethi Agarwala [1] studied the boundary layer flow over a stretching sheet in the presence of a magnetic field under velocity slip conditions. The velocity decreased with increasing slip and magnetic parameters. Furthermore Manjunatha et al [8] analyzed the free convective MHD flow of an unsteady rotating dusty fluid under the influences of a Hall current and the radiation effect.

The aim of this study was to extend the approach presented in [10] to dusty nanofluids. In [10] the authors investigated the influence of a rotating nanofluid over a stretching surface with the Richardson extrapolation method. The rotation decreases the velocity of the nanofluid. In this study the impacts of the magnetic field parameter M, mass concentration of the dust particles α and volume fraction of the nano particles ϕ on the velocity and the temperature profiles of the fluid and dust phases were investigated.

2. Mathematical Model

A steady two-dimensional laminar, MHD boundary layer flow of an incompressible dusty nanofluid past a stretching surface is considered. It is assumed that the surface z=0 is stretched by two equal and opposite forces along the x axis at a velocity of $U_w(x) = ax, a > 0$, where a is the rate of stretching. The fluid rotates with a uniform angular velocity of Ω about the z axis. In addition, a uniform magnetic field B is applied in the y direction. Both the fluid and dust particles are assumed to be static at the beginning, and the dust particles have the same size. Moreover the nano and dust particles are spherical and the relative density and volume of the dust particles are considered.

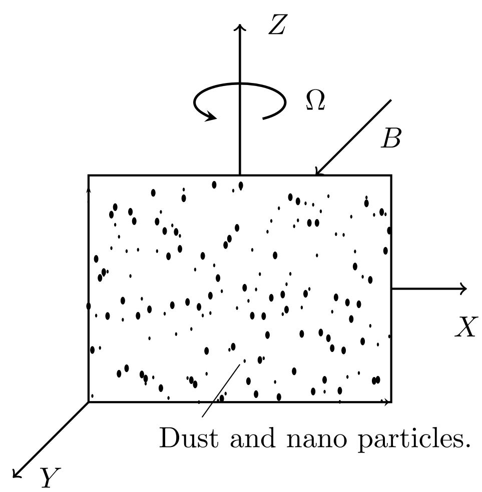

Figure 1: Configuration of problem.

The boundary layer equations that govern the present flow according to the previously presented assumptions are as follows

$$\frac{\partial u}{\partial x} + \frac{\partial v}{\partial y} + \frac{\partial w}{\partial z} = 0 \tag{2.1}$$

(2.2)
$$(1-\phi_d)\,\rho_{nf}\left(u\frac{\partial u}{\partial x}+v\frac{\partial u}{\partial y}+w\frac{\partial u}{\partial z}-2\Omega v\right)=(1-\phi_d)\,\mu_{nf}\frac{\partial^2 u}{\partial z^2}+KN\,(u_p-u)-\sigma B^2 u$$

(2.3)
$$(1-\phi_d)\,\rho_{nf}\left(u\frac{\partial v}{\partial x}+v\frac{\partial v}{\partial y}+w\frac{\partial v}{\partial z}+2\Omega u\right)=(1-\phi_d)\,\mu_{nf}\frac{\partial^2 v}{\partial z^2}+KN\,(v_p-v)-\sigma B^2 v,$$

$$\frac{\partial u_p}{\partial x}+\frac{\partial v_p}{\partial y}+\frac{\partial w_p}{\partial z}=0 \tag{2.4}$$

$$u_p\frac{\partial u_p}{\partial x}+v_p\frac{\partial u_p}{\partial y}+w_p\frac{\partial u_p}{\partial z}-2\Omega v_p=\frac{K(u-u_p)}{m} \tag{2.5}$$

$$u_p\frac{\partial u_p}{\partial x}+v_p\frac{\partial u_p}{\partial y}+w_p\frac{\partial u_p}{\partial z}-2\Omega v_p=\frac{K(u-u_p)}{m} \tag{2.6}$$

The boundary conditions in the present problem are $u = U_w = ax, v = 0, w = 0, u_p = ax, v_p = 0$ at $z = 0$, and

$$u \to 0 \qquad u_p \to 0 \qquad v_p \to v \qquad \text{as} \qquad z \to \infty \tag{2.7}$$

where (u, v, w) and (u_p, v_p, w_p) are the velocity components of the nanofluid and dust particles respectively, ϕ_d is the volume fraction of the dust particles, μ_{nf} the kinematic viscosity of the nanofluid, K the Stokes resistance, m the mass of the dust particles, N the number density of the dust particles, ρ_{nf} the density of the nanofluid, Ω the angular velocity of the rotating fluid, B the magnetic field flux density and σ the electrical conductivity. For the the next step we introduce the following set of similarity variables, including the dimensionless variable η

$$u = axf'(\eta) \qquad u_p = axF'(\eta) \qquad v = axh\,(\eta) \qquad v_p = axH\,(\eta)$$
$$w = -\sqrt{a\upsilon_f}\,f(\eta) \qquad w_p = -\sqrt{a\upsilon_f}\,F(\eta) \qquad \eta = \sqrt{\frac{a}{\upsilon_f}}z$$

where υ_f is the kinematic viscosity of the base fluid.

Equations (2.1) and (2.4) are automatically satisfied. Equations (2.2), (2.3), (2.5) and (2.6) are converted into the following ordinary differential equations:

(2.8)
$$\frac{(1-\phi_d)}{(1-\phi)^{2.5}}f'''+(1-\phi_d)\left(1-\phi+\frac{\phi\rho_s}{\rho_f}\right)\left(ff''-(f')^2+2\omega h\right)-Mf'+\alpha\beta\,(F'-f')=0$$

(2.9)
$$\frac{(1-\phi_d)}{(1-\phi)^{2.5}}h''+(1-\phi_d)\left(1-\phi+\frac{\phi\rho_s}{\rho_f}\right)(f'h-fh'+2\omega f')-Mh+\alpha\beta\,(H-h)=0$$

$$(F')^2 - FF'' - 2\omega h + \beta (F' - f') = 0 \tag{2.10}$$

$$F'H - FH' + 2\omega F' + \beta(H - h) = 0 \tag{2.11}$$

where ρ_s is the density of the copper (cu) nanoparticles, ρ_f the density of the base fluid water, (H_2O), $\alpha = Nm/\rho_f$ the mass concentration of the dust particles, $M\sigma B^2/(a\rho_f)$ the magnetic field parameter, $\beta = K/(am)$ the local fluid particle interaction parameter for the velocity, ϕ the volume fraction of the nano particles and $\omega = \Omega/a$ the non dimensional rotation parameter.

The boundary conditions in (2.7) become $f'(\eta) = 1, h(\eta) = 0, f(\eta) = 0, F'(\eta) = 1, H(\eta) = 0$ at $\eta = 0$, and

$$f'(\eta) \to 0 \qquad F'(\eta) \to 0 \qquad H(\eta) \to h(\eta) \qquad \text{as } \eta \to \infty \tag{2.12}$$

The governing heat transport equations are as follows

$$(\rho c_p)_{nf} \left(u\frac{\partial T}{\partial x} + v\frac{\partial T}{\partial y} + w\frac{\partial T}{\partial z} \right) = k_{nf}\frac{\partial^2 T}{\partial z^2} + \frac{(\rho c_p)_{nf}}{\tau_T}(T_p - T) \tag{2.13}$$

$$(\rho_p c_p) \left(u_p\frac{\partial T_p}{\partial x} + v_p\frac{\partial T_p}{\partial y} + w\frac{\partial T}{\partial z} \right) = -\frac{(\rho_p c_p)}{\tau_T}(T_p - T), \tag{2.14}$$

where T and T_p are the temperatures of the nanofluid and dust particles respectively, τ_T the thermal equilibrium time. $T_w = T_\infty + A\left(\frac{x}{l}\right)^2$ the temperature distribution in the stretching surface, where $l = \sqrt{a^{1/2}/\upsilon_f^{1/2}}$ is the characteristic length and A is a positive constant. Moreover k_{nf} is the thermal conductivity of the nanofluid, and

$$(\rho c_p)_n f \quad (\rho c_p)_f \quad \text{and } (\rho c_p)_s$$

are the volumetric heat capacities of the nanofluid, base fluid and solid nanoparticles, respectively.

The temperature boundary conditions are as follows

$$T = T_\omega \text{ at } z = 0, \text{ and } T, T_p \to T_\infty \text{ as } z \to \infty \tag{2.15}$$

where T_ω and T_∞ are the temperature values close to and far from the wall respectively.

The non-dimensional variables for obtaining the similarity solution of Equations (2.13) and (2.14) are as follows,

$$\theta(\eta) = \frac{T - T_\infty}{T_\omega - T_\infty}, \quad \theta_p(\eta) = \frac{T_p - T_\infty}{T_\omega - T_\infty} \text{ and } T - T_\infty = A\left(\frac{x}{l}\right)^2 \theta(\eta), A > 0.$$

In the next step, Equations (2.13) and (2.14) are transformed into ordinary differential equations:

$$\theta'' + \beta_T P_r (c_p)_f \left((1-\phi+\phi)\frac{\rho c_p)_s}{(\rho c_p)_f}\right)\left(\frac{k_f}{k_{nf}}\right)(\theta_p - \theta) + P_r \left((1-\phi+\phi)\frac{\rho c_p)_s}{(\rho c_p)_f}\right)\left(\frac{k_f}{k_{nf}}\right)(2f\theta' - f'\theta) = 0 \tag{2.16}$$

$$2F^{'}\theta_p - F\theta_p^{'} + \beta_T\,(\theta_p - \theta) = 0. \tag{2.17}$$

The boundary conditions (2.15) is transformed into $\theta\,(\eta) = 1$ at $\eta = 0, \theta\,(\eta) \to 0$, $\theta_p\,(\eta) \to$ as $\eta \to \infty$ where $P_r = (\mu c_p)_f / k_f$ is the Prandtl number and $\beta_T = 1/c\tau_T$ is the fluid interaction parameter for the temperature.

The nano fluid constants are as follows

$$(\rho c_p)_{nf} = (1-\phi)\,(\rho c_p)_f + (\phi)\,(\rho c_p)_s, \tag{2.18}$$

$$\frac{k_{nf}}{k_f} = \frac{(k_s + 2k_f) - 2\phi(k_f - k_s)}{(k_s + 2k_f) + \phi(k_f - k_s)}, \tag{2.19}$$

$$\mu_{nf} = \frac{\mu_f}{(1-\phi)^{2.5}}, \tag{2.20}$$

$$(\rho)_{nf} = (1-\phi)\,(\rho)_f + \phi\rho_s \tag{2.21}$$

where μ_f is the dynamic viscosity of the base fluid and k_f and k_s are the thermal conductivities of the base fluid and nanoparticles respectively.

The local skin friction coefficients in the x and y directions and the local Nusselt number can be expressed as $Cf_x = \tau_{xz}/(\rho_f(ax))^2, Cf_y = \tau_{yz}/(\rho_f(ax))^2$, and $Nu_x = xq_w/(k_f(T_\omega - T_\infty)$ where the shear stresses of the x and y component $\tau_{xz}, \tau_{yz}, q_w$ are as follows

$$\tau_{xz} = \mu_{nf}(\frac{\partial u}{\partial z})_{z=0} \qquad (Re_x)^{1/2} Cf_x = \frac{1}{(1-\phi)^{2.5}} f''(0)$$

$$\tau_{yz} = \mu_{nf}(\frac{\partial v}{\partial z})_{z=0} \qquad (Re_x)^{1/2} Cf_y \frac{1}{(1-\phi)^{2.5}} h'(0)$$

$$q_w = -k_{nf}(\frac{\partial T}{\partial z})_{z=0} \qquad (Re_x)^{-1/2} Nu_x = \frac{-k_{nf}}{k_f}\theta'(0),$$

where $Re_x = \frac{xU_w}{\upsilon_f}$, is the local Reynolds number and Nu_x is the local Nusselt number.

3. Results and Discussions

The coupled nonlinear ordinary differential equations (2.8), (2.9), (2.10),(2.11), (2.16) and (2.17) with boundary conditions (2.12) and (2.18) were solved numerically with the MATLAB bvp4c algorithm. The following values were maintained throughout the study except the varied values shown in the graphs and table.

$$\phi_d = 0.1, \phi = 0.1, \alpha = 1, \beta = 1, P_r = 6.2, M = 1 \text{ and } \beta_T = 0.3.$$

We considered $Cu - H_2O$ as the nanofluid embedded with conducting dust particles.

	$\rho(Kgm^{-3)}$	$c_p(JKg^{-1}K^{-1})$	$k(Wm^{-1}K^{-1})$
H_2O	997.1	4179	0.613
Cu	8933	385	401

Table 1: Thermo physical properties of base fluid H_2O and nanoparticle Cu

P_r	Previous studies	Present study
1	1.3333	1.333333333
3	2.5097	2.509725227
10	4.7969	4.796853285

Table 2: Comparison of results of temperature gradient $-\theta'(0)$ to results in previous studies [7, 13, 14]

Table 2 shows the effect of different Prandtl numbers Pr on the heat transfer rate. The results agree well with those published in [7, 13, 14]. Figure 2 shows the effect of the rotation parameter ω on the velocity and temperature profiles of the fluid and dust phases. The velocites along the x axis of the fluid and dust phases increase with increasing value of ω. By contrast, the velocities along the y axis of the fluid and dust phases decrease with increasing ω. Thus, an increasing ω intensifies the temperature profiles of the fluid and dust phases. Moreover, Figure 3 presents the impact of the mass concentration of the dust particles α on the velocities along the x and y axes and the temperature profiles of the fluid and dust phases. The increasing αdecreases the velocity and temperature profiles of the fluid and dust phases. In other words, an increasing mass concentration of the dust particles increases the weight of the dust phase, which slows down the velocity and temperature profiles. Figure 4 presents the influence of the magnetic field parameter M on the velocity and temperature profiles of the fluid and dust phases. The increasing magnetic field parameter decreases the velocities of the fluid and

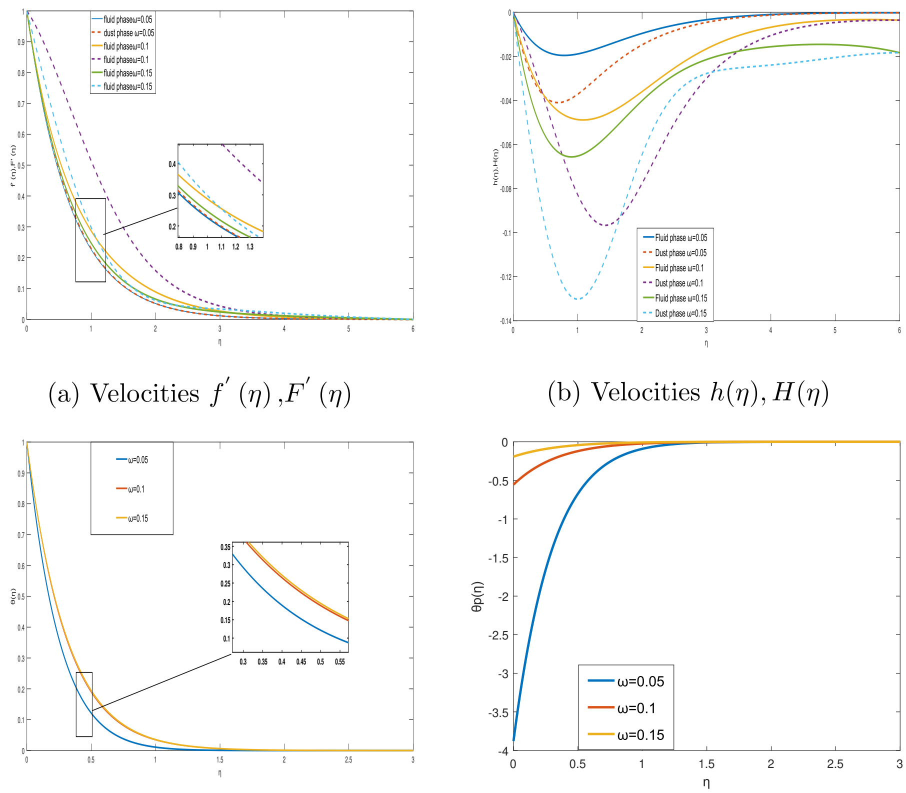

(a) Velocities $f^{'}(\eta)$,$F^{'}(\eta)$ (b) Velocities $h(\eta), H(\eta)$

(c) Temperature $\theta(\eta)$ (d) Temperature $\theta_p(\eta)$

Figure 2: Effect of ω on velocity and temperature

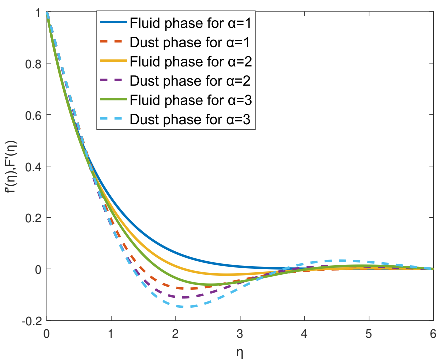

(a) Velocities $f'(\eta), F'(\eta)$

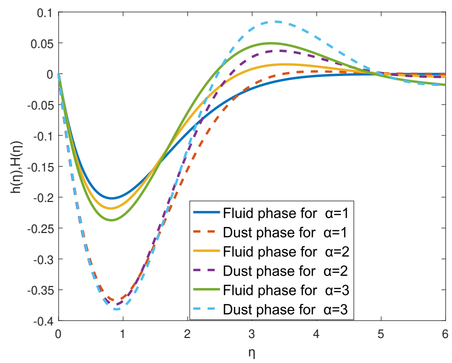

(b) Velocities $h(\eta), H(\eta)$

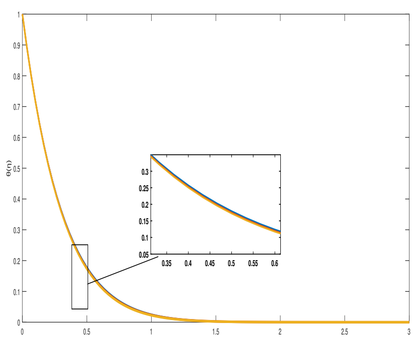

(c) Temperature $\theta(\eta)$

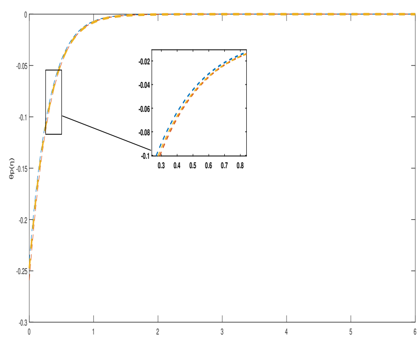

(d) Temperature $\theta_p(\eta)$

Figure 3: Effect of α on velocity and temperature

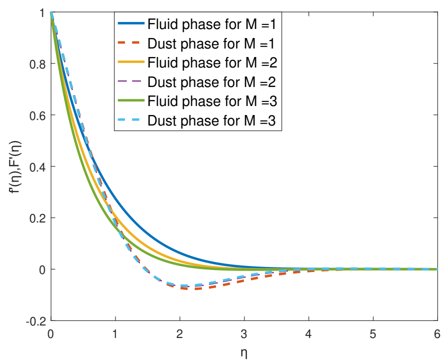

(a) Velocities $f'(\eta), F'(\eta)$

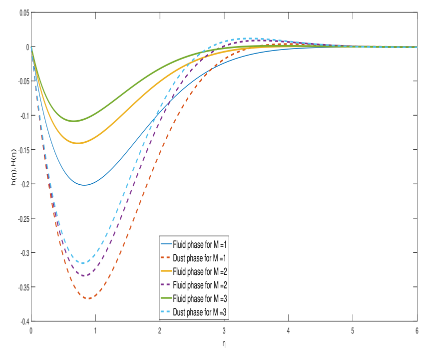

(b) Velocities $h(\eta), H(\eta)$

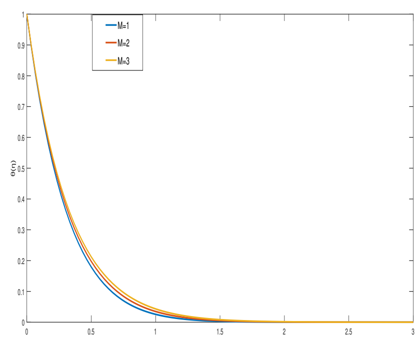

(c) Temperature $\theta(\eta)$

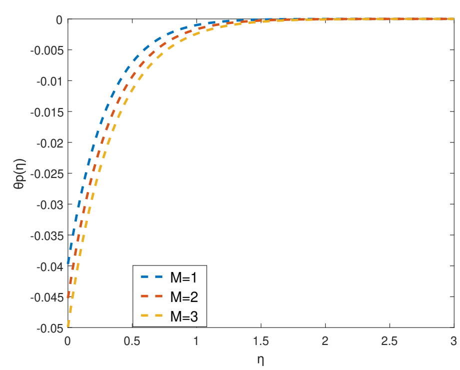

(d) Temperature $\theta_p(\eta)$

Figure 4: Effect of M on velocity and temperature

dust phases along the x axis because the magnetic field force acts in the opposite direction with respect to that of the flow. Nevertheless, the magnetic field increases the velocities of the fluid and dust phases along the y axis because it is applied in the y axis direction. The magnetic field parameter increases with the thermal boundary layer thickness; in addition, it increases the temperature of the fluid flow and decreases the temperature of the dust phase. Figures 5 describes the effects of the fraction by volume ϕ of the nano particles on the velocity and temperature profiles of the fluid and dust phases. Evidently, an increasing ϕ decreases the velocity profiles of the fluid and dust phases along the x axis and the temperature profile of the dust phase. The opposite trend is shown in the velocity profiles along the y axis and temperature profile of the fluid phase. Figures 18-20 show the variations in the local skin friction coefficient along the x and y axes and the local Nusselt number for different ϕ. With increasing volume fraction of the nanoparticles, the local skin friction coefficients along the x and y axes decrease, whereas the local Nusselet number increases.

Table 3. shows the effects of different M, α, β, ϕ, and ϕ_d on the friction factor and heat transfer rate.

ϕ	M	α	ω	f"(0)	h'(0)	-θ '(0)
0.1	1	1	**0.05**	-1.489798495	-0.06294225	3.954504366
0.1	1	1	**0.1**	-1.508698003	-0.133077626	3.271078881
0.1	1	1	**0.15**	-0.709133996	-0.054132233	3.202471601
0.1	1	**1**	0.5	-1.376859142	-0.628359567	3.236010696
0.1	1	**2**	0.5	-1.386452123	-0.664324882	3.252656071
0.1	1	**3**	0.5	-1.378351797	-0.697723093	3.265149741
0.1	**1**	1	0.5	-1.376859142	-0.628359567	3.236010696
0.1	**3**	1	0.5	-1.90404752	-0.447532061	3.103644548
0.1	**5**	1	0.5	-2.324503788	-0.364571756	3.111346713
0.1	1	1	0.5	-1.376859159	-0.628359593	3.235959697
0.2	1	1	0.5	-1.296596287	-0.703943407	2.665773659
0.3	1	1	0.5	-0.813184737	-1.347880625	2.190351303

Table 3: Variation in $f''(0), h'(0)$ and $\theta'(0)$

Conclusion

The fluid flow and heat transfer of a rotating dusty nanofluid on a stretching sheet was numerically investigated. The studied $Cu - H_2O$ nanofluid contained conducting dust particles. The governing equations of the flow and heat transfer of the dusty nanofluid were reduced in a similarity analysis and solved with the MAT-

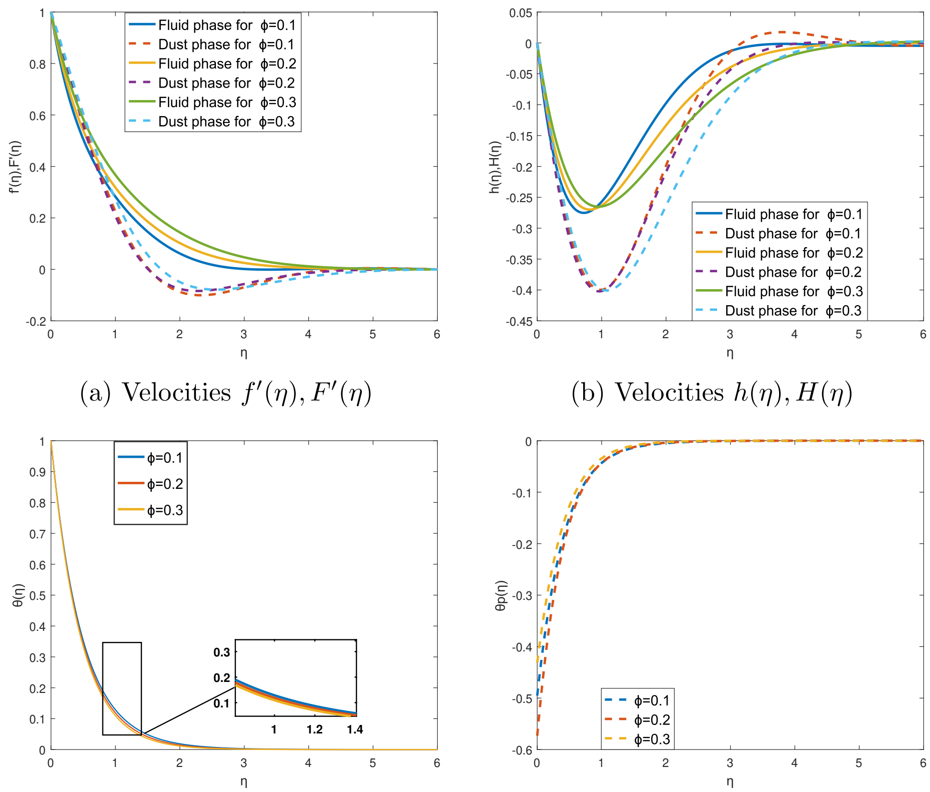

(a) Velocities $f'(\eta), F'(\eta)$

(b) Velocities $h(\eta), H(\eta)$

(c) Temperature $\theta(\eta)$

(d) Temperature $\theta_p(\eta)$

Figure 5: Effect of ϕ on velocity and temperature

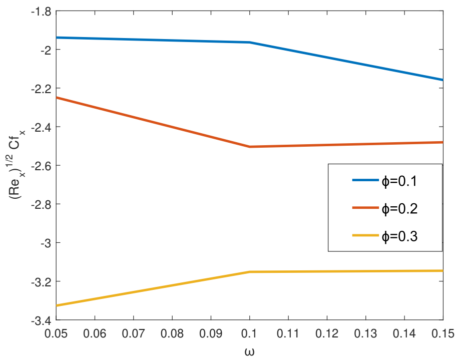

(a) Skin friction along x axis

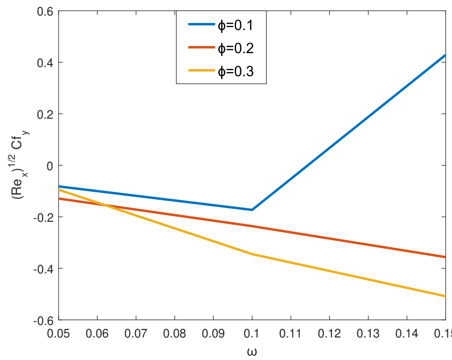

(b) Skin friction along y axis

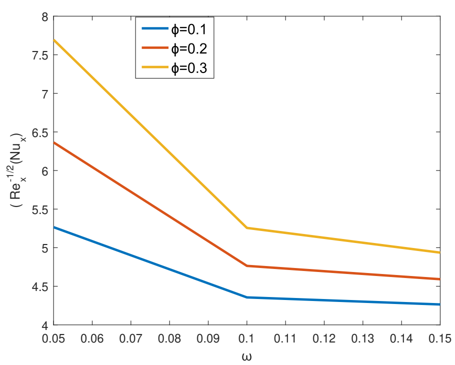

(c) Local Nusselt Number

Figure 6: Variations in skin friction and local Nusselt number

LAB bvp4c algorithm. Finally, the effects of different non-dimensional parameters on the velocity and temperature profiles of the fluid and dust phases were plotted and analyzed. The following conclusions were drawn:

- The fluid and dust phases exhibit increasing temperature profiles.
- An increasing volume fraction of the nano particles ϕ decreases the friction factors along the x and y axes.
- An increase in the volume fraction of the nano particles ϕ increases the local Nusselet number.
- The temperature gradient for different Prandtl number Pr agrees with those of other papers.

References

[1] P. Agarwala and R. Khare, *MHD flow of Cu-water nanofluid over a stretching sheet with second order slip condition*, Int. J. Sci. Eng. Res., **6(5)**(2015), 895–904.

[2] S. U. S. Choi, *Enhancing thermal conductivity of fluids with nano particles*, International Mechanical Engineering Congress and Exposition, **66**(1995), 99–105.

[3] L. J. Crane, *Flow past a stretching plate*, Zeitschrift für angewandte Mathematik und Physik, **21**(1970), 645–647.

[4] M. Ferdows, S. M. Chapal and A. A. Afify, *Boundary layer flow and heat transfer of a nanofluid over a permeable unsteady stretching sheet with viscous dissipation*, J. Eng. Thermophys., **23**(2014), 216–228.

[5] B. J. Gireesha, B. Mahanthesh and R. S. Reddy Gorla, *Suspended particle effect on nanofluid boundary layer flow past a stretching surface*, J. Nanofluids, **3**(2014), 1–11,

[6] B. J. Gireesha, G. K. Ramesh, H. J. Lokesh and C. S. Bagewadi, *Boundary layer flow and heat transfer of a dusty fluid over a stretching vertical surface*, Appl. Math., **2**(2011), 475–481.

[7] L. J. Grubka and K. M. Bobba, *Heat transfer characteristics of a continuous, stretching surface with variable temperaturer*, J. Heat transfer, **107**(1985), 248–250.

[8] S. Manjunatha, B. J. Gireesha and C. S. Bagewadi, *Series solutions for an unsteady flow and heat transfer of a rotating dusty fluid with radiation effect*, Acta Math. Univ. Comenian., **86(1)**(2017), 111–125.

[9] J. C. Maxwell, *A treatise on electricity and magnetism*, 3^{rd}ed., Oxford University Press, London, 1892.

[10] S. Nadeem, A. U. Rehman and R. Mehmood, *Boundary layer flow of rotating two phase nanofluid over a stretching surface*, Heat Transfer, **45**(2014), 285–298.

[11] S. Naramgari and C. Sulochana, *MHD flow of dusty nanofluid over a stretching surface with volume fraction of dust particles*, Ain Shams Eng. J., **7**(2016), 709–716.

[12] B. C. Sakiadis, *Boundary layer behavior on continuous solid surfaces. II. Boundary layer on a continuous flat surface*, J. Amer. Inst. Chem. Eng., **7**(1961), 221–225.

[13] N. F. Md Shab and A. Anati, *Hydromagnetic boundary layer flow of a dusty fluid in a porous medium over a stretching sheet with slip effect*, Malaysian J. Fund. Appl. Sci., **13(3)**(2017), 170–173.

[14] M. I. Sharena, A. Anati and S. Sharidan, *Magnetohydrodynamic flow of dusty fluid past a vertical stretching sheet with hall effect*, AIP Conference Proceedings **1750**, (2016), 020005.